

Design of a Magnet Assembly for an NMR Based Sensor Using Finite Element Analysis

S. I. Cho, C. H. Chung, S. C. Kim

Abstract: A magnet assembly is a critical element of a nuclear magnetic resonance(NMR) based sensor. Magnetic flux density and homogeneity are essential to its optimum performance. Geometry and magnet material properties determine the magnetic flux density and homogeneity of the assembly. This study was carried out to develop the design for a magnet assembly. A 2-D finite element model for the magnetic assembly was developed using ANSYS and evaluated the effects of adding shimming frames and steel bars in the corners of the rectangular steel cover which surrounded the magnet. The assembly was manufactured and evaluated. According to the ANSYS model, modified pole frames increased magnetic flux density by 8.3% and increased homogeneity by 83%. Addition of steel bars in the corners increased the magnetic flux density by 1%, and improved homogeneity up to three times. The difference between simulated and measured magnetic flux densities at the center point of the air gap was within 2.4%.

Keywords: NMR, Magnet Assembly, Finite Element Model, Homogeneity

Introduction

Non-destructive quality measurement of agricultural products is a crucial research area in agriculture. Optics, NIR spectroscopy, ultrasonic testing and imaging, and NMR spectroscopy are the state-of-art technologies which are being evaluated for use in non-destructive quality sensors(Brusewitz, 1987; Cho, 1988; Bray, 1992). Specially, proton (^1H) NMR is one of the most powerful techniques in chemical analysis. Non-destructive qualitative and quantitative analysis are possible based on the resonant absorption and emission of magnetic energy of protons subjected to a magnetic field (Martin, 1980).

The NMR-based sensor consists of a magnet assembly, probe and electronic circuits. Among the components of NMR sensor, magnet assembly is a basic element which produces the fixed magnetic field. Usually, a super-conducting magnet is used in NMR equipment designed for medical imaging or chemical analysis. A permanent magnet having a magnetic field strength of about 1,000 to 4,000 gauss can be used for NMR-based agricultural sensors.

The proper design of a magnetic assembly using the permanent magnets is important to get desired magnetic flux density (B) and its homogeneity. Cho et al. (1990) used a the finite element analysis method to design magnet assembly about 1,000 gauss. They proposed a design using pole faces and shimming frames to enhance the homogeneity. However, the

homogeneity was not good enough for the NMR-based sensors. If the homogeneity is larger, then more sensing information from the NMR-based sensor is lost. Therefore, enhancing the homogeneity is important for the sensor.

The goal of this study is to design the magnet assembly having good homogeneity. The detailed objectives were 1) to find out design factors to enhance the homogeneity, 2) to utilize the ANSYS for the design process, and 3) to evaluate the manufactured magnetic assembly.

Materials and Methods

1. Geometry of Magnet Assembly

Magnet assembly configuration can be classified into two categories: box and cylindrical. A box type assembly was designed(fig. 1) and the geometry of the magnet assembly was specified using 10 design variables. Descriptions of each parameter are listed in table 1.

The influence of each parameter on magnetic flux density and homogeneity was studied. The Magnet assembly was designed by considering the size of fruits such as apple, kiwi etc., for test and its parameters were slightly changed by the result of simulations. The dimension of the air gap, where agricultural products would be located, was constraint in the design. Pole frame and triangular steel bars(i) in the corners of the rectangular steel cover were proposed to enhance magnetic flux density and homogeneity of the magnet assembly.

The distribution of magnetic flux density was studied in two planes. One plane(X-Z plane, fig. 1 (a)) was located along the center line of the magnet assembly and parallel to the assemblies open faces. The second plane(Y-Z plane, fig. 1 (b)) was along the center line which was perpendicular to the open faces.

The authors are **Seong In Cho**, Associate Professor, **Chang Ho Chung**, Research Assistant, **Seung Chan Kim**, Research Assistant, School of Bioresources and Materials Engineering, College of Agriculture and Life Sciences, Seoul National University, Korea. **Corresponding author:** Seong In Cho, Associate Professor, School of Bioresources and Materials Engineering, College of Agriculture and Life Sciences, Seoul National University, Suwon 441-744, Korea; e-mail:sicho@snu.ac.kr.

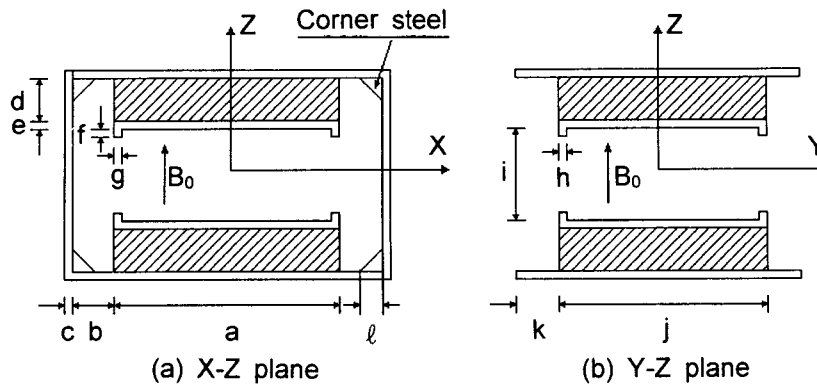


Fig. 1 Magnet assembly configuration (box type).

Table 1 Design parameters and specifications for the magnet assembly

Variable	Descriptions	Specifications (mm)
a	Total width of magnet	304.8
b	Horizontal space gap (X-Z)	38.1
c	Thickness of steel cover	25.4
d	Thickness of magnet	76.2
e, f, g, h	Shape of pole frame	12.7, 12.7, 12.7, 12.7
i	Air gap	152.4
j	Total length of magnet	304.8
k	Horizontal space gap (Y-Z)	38.1
l	Thickness of corner steel (X-Z)	Varied

The performance of magnet assembly for the NMR-based sensor was evaluated by its magnetic flux density and homogeneity.

An MG-40 Gaussmeter (Walkers scientific, Inc.; ±0.05% error) was used to measure the magnetic flux density. The homogeneity of the magnetic field was calculated using equation (1).

$$\begin{aligned}
 \text{Homogeneity} &= \frac{\text{Maximum deviation of magnetic fields}}{\text{Average magnetic field}} \times 10^6 [\text{ppm}] \\
 &= \frac{|\Phi_i - \Phi_{\text{avg}}|_{\text{max}}}{\Phi_{\text{avg}}} \times 10^6 [\text{ppm}] \quad (1)
 \end{aligned}$$

where, Φ_i is a magnetic flux density at one point and Φ_{avg} is a average magnetic field

2. Design of the Magnet Assembly using Finite Element Analysis

The finite element method has been a powerful tool for solving problems in areas of research such as statics, dynamics, thermodynamics and fluid dynamics.

Electromagnetics problem also be solved using the finite element method. Many commercial finite element packages, such as ABAQUS, NASTRAN, FLUENT, and ANSYS, are available. ANSYS(SASI-Swanson Analysis System, Inc.) 5.0 for the SunSparc Workstation was used for the design of the magnet assemblies.

3. Finite Element Model for Permanent Magnet

The governing equations for the finite element model were Maxwell's equations for electromagnetic field analysis.

$$\begin{aligned}
 \nabla \times \vec{H} &= \vec{J} \\
 \vec{B} &= \nabla \times \vec{\Phi} = \mu \cdot \vec{H} \\
 \nabla \times \vec{\Phi} &= 0 \quad (2)
 \end{aligned}$$

$$\text{where, } \nabla = \vec{i} \frac{\partial}{\partial x} + \vec{j} \frac{\partial}{\partial y} + \vec{k} \frac{\partial}{\partial z}$$

4. Permanent Magnet Materials

The choice of material for the permanent magnet affects the cost and performance of the magnet assembly. Nd-Fe-B, rare earth or ceramic magnet materials could be used. Ferrite (or ceramic 8, by which it is referred to hereafter) permanent magnet was chosen. Because it is relatively light and inexpensive. The properties of a permanent magnet are described using μ (magnetic permeability) and the demagnetization curve (B-H curve), The relation between magnetic flux density (B) and field intensity (H) is non-linear. Fig. 3 shows the demagnetization curves of the ferrite permanent magnet and the low carbon steel at ambient temperature(20°C).

Results and Discussion

1. Design Program for Finite Element Analysis

ANSYS includes APDL (ANSYS Parametric Design Language) which makes it easy to modularize, modify

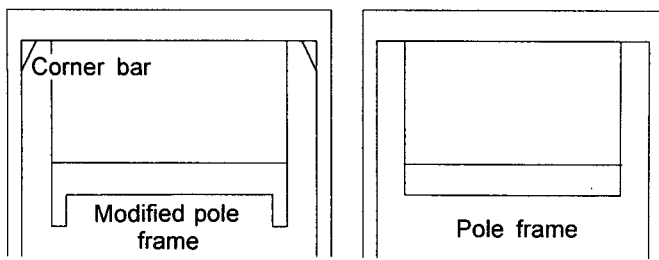


Fig. 2 Two kinds of magnet assembly; left: with modified pole frame and corner steel; right: with pole frame.

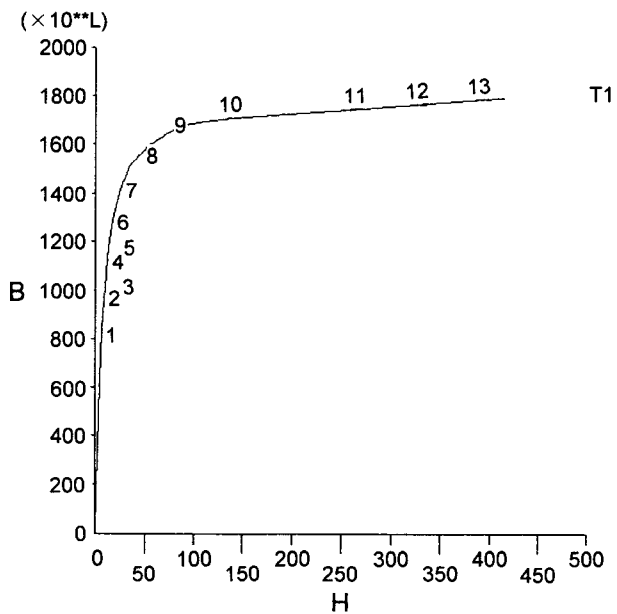
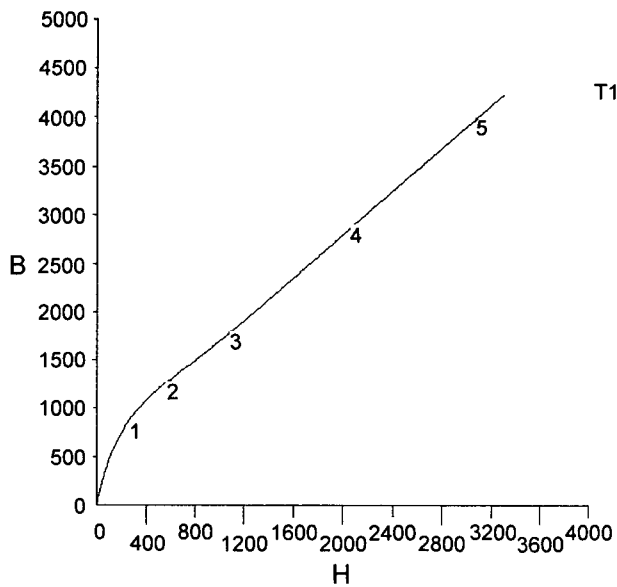


Fig. 3 Demagnetization curves(left: magnet, right: steel).

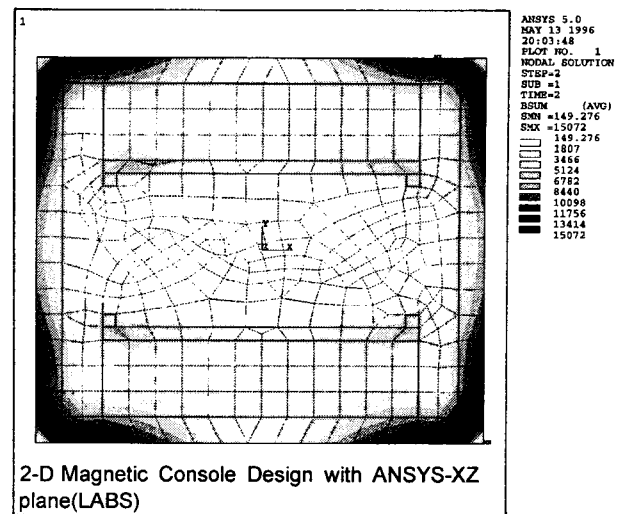


Fig. 4 Post-processing output showing magnetic flux density in scalar quantities.

and update the analysis procedures. Pre-processing (modeling and mesh generation), solution, and post-processing module were developed. 2-D models for both the X-Z plane and the Y-Z plane were used for the analysis. Fig. 4 shows the magnetic flux density in scalar quantities obtained from the post-processing module.

2. Validation of Finite Element Analysis for Magnet Assembly

The results of a finite element analysis should be validated using the measurements on manufactured prototypes. Several prototype magnet assemblies were manufactured from Ceramic 8 magnet material and measurements on these assemblies were compared with the result of the finite element analysis. Magnetic flux density, which is dependent upon temperature, was measured at 21.5°C while a temperature of 20°C was assumed for the model. The magnetic flux density is dependent upon its temperature. The field intensity of the Ceramic 8 magnet decreases 0.19% for each 1°C increase in temperature(Tabble and Craik, 1969).

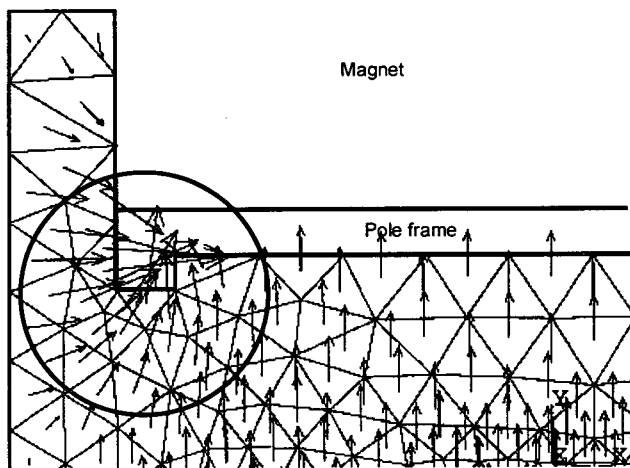
Table 1 shows the specification of the prototype magnet assembly which was used to validate the ANSYS simulation. Comparisons of measured values with predicted values are shown in table 2. Homogeneity was calculated within for a spherical region having a diameter of 25mm and centered in the air gap. The difference between measured and predicted values was 26 gauss. The error was about 3%, the 1.5°C temperature difference.

Geometry of the magnet assembly had a significant influence on the magnetic flux density and homogeneity. The optimum values of each part were searched to enhance the homogeneity of the magnet assembly by the trial and error method. As a result

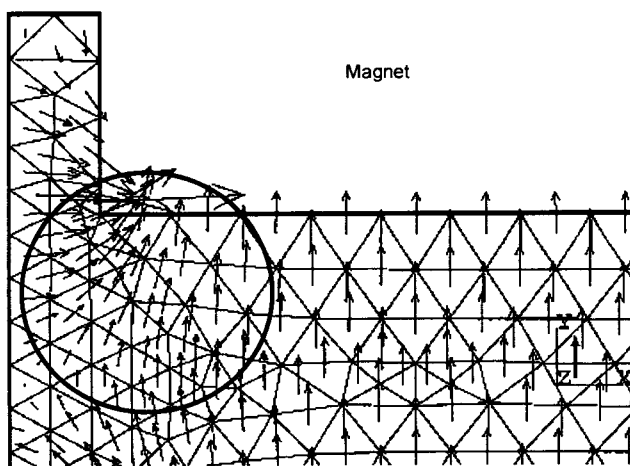
Table 2 Comparison of measured values with predicted values for the magnet assembly with modified pole frame

	Magnetic flux density (gauss)	Homogeneity (ppm)	
Measured	988 *	1015 (X-Z)	1015 (Y-Z)
Predicted	959	1196 (X-Z)	397 (Y-Z)

* Value was corrected for the temperature difference between magnet temperature(21.5°C) and the temperature assumed in the ANSYS model(20°C)



(a) with the pole frame



(b) without the pole frame

Fig. 5 Vector plot of magnet flux in the vicinity of the corner of the magnet: (a) with and (b) without the pole frame.

of the optimization, $d=20.0$ mm and $k=17.8$ mm with other values remaining unchanged. The homogeneities were improved from 1,196 ppm to 345 ppm (X-Z) and from 397 ppm to 116 ppm (Y-Z). However the magnetic flux density was reduced from 959 gauss to 956 gauss.

3. Effects of Pole Frame and Corner Bar

The pole frame and corner bars were adapted to enhance the homogeneity of the magnet assembly. It was anticipated that the modified pole frame would bend the magnetic flux inward, thereby reducing the loss of magnetic flux at the outer part of the air gap as shown in fig. 5.

To verify the effect of the modified pole frame, the magnet assembly was also analyzed. The result, compared with the magnet assembly having a pole frame, shown in table 3. The modified pole frame reduced the average magnetic flux density by 8.3% and improved the homogeneity by 75.2% (X-Z) and 97.6% (Y-Z). To recover the reduction in magnetic flux density, the thickness (d), length (g), or width (a) of the permanent magnet material should be adjusted. To minimize the effect on the homogeneity, the increase in magnet flux density was achieved by increasing the thickness of the magnet. The result is shown in table 4.

The rectangular outer steel cover formed a closed circuit for the magnetic field. Because of the rectangular shape, the magnetic field was concentrated at each corner and magnetic flux density peaked. This decreased the homogeneity at the center of the air gap. It was anticipated that the corner bars would reduce the concentration of the magnet field at each corner without affecting the magnetic flux density at the center of the air gap. As shown in table 5, installation of corner bars at each corner, but increased magnetic flux density at the center of air gap from 956 to 962, and increased homogeneity to 103 ppm (X-Z plane). Comparison result is shown in table 5.

Conclusions

A magnet assembly is a critical element for an NMR based sensor and its homogeneity has a major effect on the performance of the sensor. The magnetic flux density and homogeneity of the assembly are dependent upon geometry and material properties. Therefore, it is necessary to develop the optimum design using computer simulations.

This study used a two dimensional ANSYS finite element model to reduce the design error estimated to be. The error between the value at the center point a determined from the model and the measured value of magnetic field intensity was 2.64%.

Pole frames and corner bars were proposed as method of enhancing the magnetic flux density and

Table 3 Comparison of the magnet assembly with pole frame

Pole frame	Magnetic flux density (gauss)			Homogeneity (ppm)	
Modified pole frame	1,242(X-Z)	669(Y-Z)	956 (average)	345(X-Z)	116(Y-Z)
Pole frame	1,363(X-Z)	723(Y-Z)	1,043 (average)	1,392(X-Z)	4,776(Y-Z)

Table 4 Changes of magnetic flux density and homogeneity with increases in thickness of the material assembly (d=20.3 mm, k=17.8 mm)

Thickness (mm)	Magnetic flux density (gauss)			Homogeneity (ppm)	
76.2 (Original)	1,242(X-Z)	669(Y-Z)	956	345(X-Z)	116(Y-Z)
83.8 (+10%)	1,354(X-Z)	712(Y-Z)	1,033	324(X-Z)	338(Y-Z)
91.4 (+20%)	1,386(X-Z)	751(Y-Z)	1,069	339(X-Z)	355(Y-Z)

Table 5 Comparison of magnet flux density and homogeneity of the magnet assembly "with" and "without" corner bar

Corner steel	Magnetic flux density (gauss)		Homogeneity (ppm)	
Installed	962**		103***	
Not installed	956**		345***	

** : These values were averaged with flux density of X-Z plane and Y-Z plane

*** : These values were the homogeneity at only X-Z plane

homogeneity of the magnet assembly. The ANSYS model results indicated that adaptation of modified pole frames increased magnetic flux density at the center point by 8.3% and increased the magnetic field homogeneity by 86%. And the corner bars increased magnetic flux density by less than 1%, but improved the homogeneity by 300%. Therefore, the pole frame and the corner bar are crucial to achieve maximum performance of the magnet assembly.

References

- Brusewitz, H. H. and M. L. Stone. 1987. Wheat moisture by NMR. Transactions of the ASAE 30(3): 858-862.
- Bray, D. E. and D. McBride. 1992. Nondestructive Testing Techniques. John Wiley & Sons, Inc.
- Cho, S. I. 1988. Development of nuclear magnetic resonance based sensor to detect ripeness of fruit. Unpublished Ph.D. thesis. Agricultural Engineering Dept. Purdue University. W. Lafayette, IN.
- Cho, S. I., G. W. Krutz, H. G. Gibson and K. Haghghi. 1990. Magnet assembly design of an NMR-based sensor to detect ripeness of fruit. Transactions of the ASAE 33(4):1043-1050.
- Martin, M. L., J. -J. Delpuech and G. J. Martin. 1980. Practical NMR Spectroscopy. Heyden.
- SASI. 1992. ANSYS 5.0 User's Manual. Swanson Analysis Systems, Inc.
- Tabble, R. S. and D. J. Craik. 1969. Magnetic Materials. John Wiley & Sons, Ltd, pp 451-455.